

Effect of Graphite Electrode to Surface's Characteristic of EDM

Apiwat Muttamara¹, Warunee Borwornkiatkaew², Anuprong Pronpijit² and Songkran Nuanchom²

¹Faculty of Engineering, Thammasat University, Pathum Thani 12120, Thailand

²National Metal and Materials Technology Center (MTEC), Pathum Thani 12120, Thailand

Abstract. Electrical discharge machining process (EDM) is a process for removing material by the thermal of electrical discharge. Some of the melted and all of the evaporated material is then quenched and flushed away by dielectric liquid and the remaining melt recast on the finished surface. The recast layer is called as white layer. Beneath the recast layer, a heat affected zone is formed. The quality of an EDM product is usually evaluated in terms of its surface integrity, which is characterized by the surface roughness, existence of surface cracks and residual stresses. This paper presents a study of surface's characteristics by EDM in de-ionized water due to decarbonisation. The machining tests were conducted on mild steel JIS grade SS400 with copper and graphite electrodes. The workpiece surfaces are analyzed by scanning electron microscope and XRD technique. The carbon transfers from graphite electrode to the white layer relating to martensitic phrase of recast layer.

1 Introduction

Electrical Discharge Machining (EDM) is one of the most effective methods for removing material from electrical conductive materials. When machining a workpiece with EDM, a recast layer is formed at the surface of the workpiece [1]. The recast layer shows white color after etching so it is called the white layer. The white layer is the result of the solidification of a melted zone and is known to exhibit high hardness, good adherence to the bulk and good resistance to corrosion. However, it contains a lot of microcracks, which causes a problem for certain applications. The microstructure and the properties of the melted zone after solidification are quite different with respect to those of the workpieces and tool electrodes used in de-ionized water [2]-[5]. EDM process can be performed in decarbonization for example EDM process in deionized water. Graphite is widely used as electrode material in EDM, this is due to its low density and good electrical along with its machinability [5]-[6]. This research was studied the effect of electrode to EDM process in deionized water.

2 Experimental

The machine used for this study is a FORM 2-LC of Charmilles Technologies. From the previous studies of Lee et al. [7], they used the Taguchi approach and found that the characteristics of an EDMed surface, such as surface roughness and white layer thickness are mainly influenced by current and discharge duration.

Decarbonisation is interesting for the experiment in order to observe carbon in electrode material affect to the surface's characteristics. Thus this study was carried out in de-ionized water and also used the EDM conditions for examining the characteristics of an EDMed surface. The workpieces was mild steel (SS400). Electrodes are copper and graphite, diameter of 12 mm. The properties are shown in Table 1. The parameters are shown in Table 2. The formation of surface cracks was checked by scanning electron microscope and the structural phrases were analysed by X-ray diffraction (XRD).

Graphite is the preferred electrode material because light weight and easy for machining. Graphite was made by compressing the powder/binder mixture in only one direction, resulting in grain relate to impact force direction. Graphite has significantly lower mechanical strength properties than metallic electrode ex. copper. It is neither as hard as strong, nor ductile as copper electrode. Due to the significant differences between copper and graphite electrode, the study was carried out in water di-electric fluid.

Table 1. Properties materials.

Properties	Value
Thermal Conductivity (W/m°C)	53.66
Density (g/cm ³)	7.85
Melting point (°C)	1,495
Young's Modulus (GPa)	400

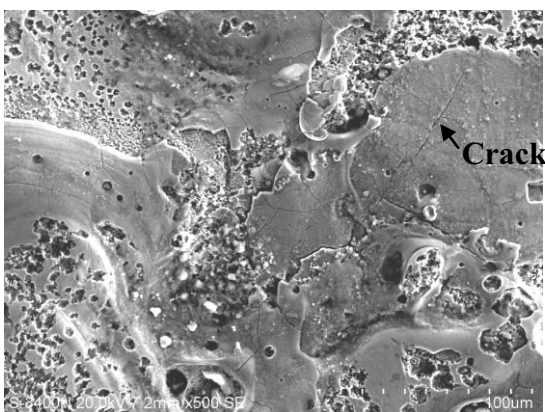
Table 2. EDM conditions.

Properties	Value
Polarity	Negative
Open Load Voltage (Volts)	250
Current (A)	5-30
Discharge duration (μ s)	300
Duty Factor (%)	50

3 Results and Discussions

The machined workpiece surfaces were observed by scanning electron microscope (SEM) as shown in Fig. 1. The machined surface were treated with copper (Fig.1(a)) and graphite electrode (Fig.1(b)). Some micro-cracks were found on the EDMed surface when using a copper electrode, but no crack was observed when using a graphite electrode. This may explain that powder from graphite electrode easily drop to recast layer during discharge process. Consequently, the recast layer contains many holes and channels caused by the bubble air that generated during EDM process. The copper electrode gives more small pores and hole compared to graphite electrode. The recast layer also contained some microcracks. The heat from EDM process melts and evaporates the workpiece material. The treated surface is covered with debris and voids because of the high heat energy released by the electrical discharges, followed by rapid cooling. It seems that the copper electrode generated more bubble air than that of the graphite electrode [8]. However, graphite is a powder / sintering material by compressing. The graphite does not melt absolutely, but sublimates from an electrode during discharge.

a) SS400 with copper electrode



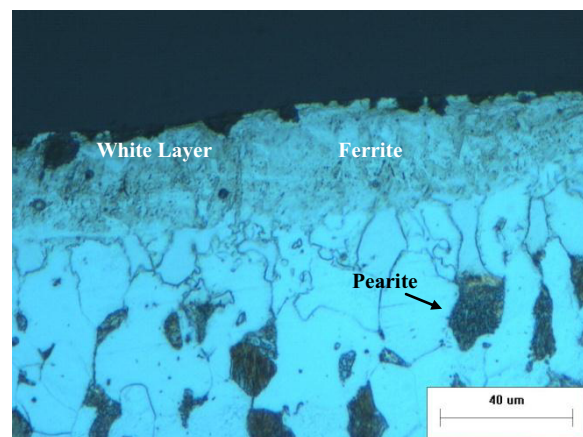
b) SS400 with graphite electrode



Figure 1. SEM image of EDMed surface machined on SS400 with (a) copper and (b) graphite electrode.

Fig. 2 (a) shows a cross-sectional image of etched SS400 with copper electrode. Fig. 2 (b) shows a cross-sectional etched SS400 with graphite electrode. During the solidification, as the temperature drops near the eutectic temperature it tends to transform into ferrite, carbide and retained austenite.

a) SS400 with copper electrode



b) SS400 with graphite electrode

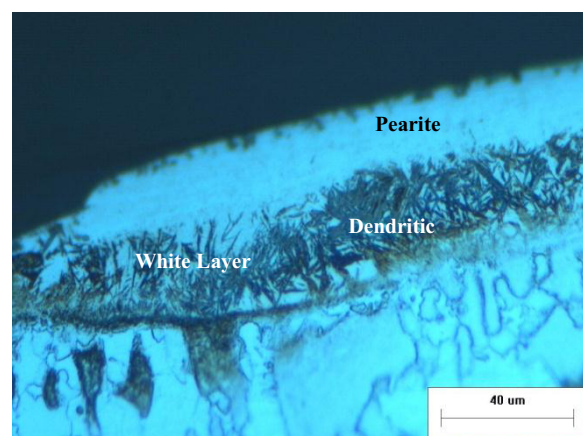
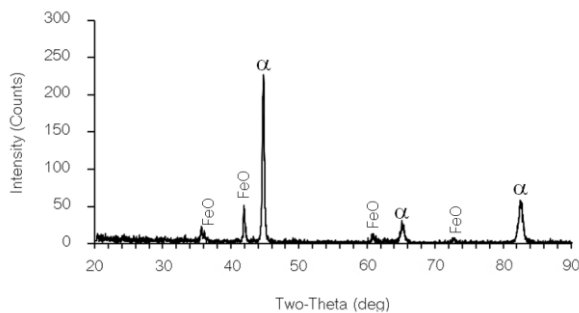


Figure 2. Cross-sectional of EDMed surface for SS400 with (a) copper and (b) graphite electrode ($I=25$ A, $t_{on}=300$ μ s)

Now we can determine that quench is rapid enough to precipitate carbides in martensite structure formed in the white layer in Fig. 2 (b). A thin columnar dendritic sublayer is observed on the recast layer. This reveals the phases consisting of martensite and residual austenite with dendritic structure [9-12]. Beneath the recast layer is a sublayer that is not melted called the heat affected zone (HAZ). The matrix of the workpiece is composed of pearlite and ferrite.

Fig. 8 displays XRD patterns of SS400 with copper and graphite electrode. The result shows iron oxides and α -Fe in the recast layer in Fig. 8(a). FeO came from chemical reaction between the workpiece and elemental oxygen decomposed from the deionized water during sparking [13]. Fig. 8(b) shows the XRD pattern with graphite electrode. Some carbon was found in the recast layer. However, we did not detect the presence of Fe_3C or any composed carbon with iron, so their contents in the recast layer were low.

a) SS400 with copper electrode



b) SS400 with graphite electrode

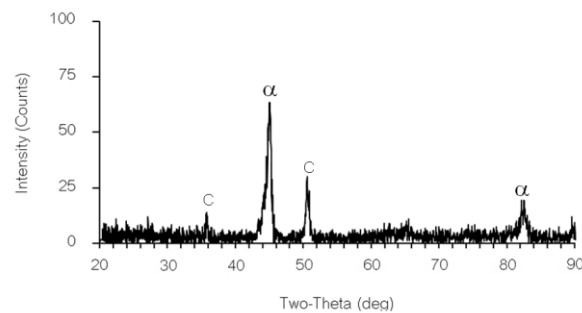


Figure 3. XRD patterns of surfaces treated by EDM with a) copper and b) graphite electrodes.

To study the characteristics of the material phases, the microhardness of the recast layer of each sample was also measured at different distances from the top layer. The comparison shown in Fig.4 denotes compares the microhardness of the cross section of the recast layers of different electrode materials: graphite and copper. A low load of 10 gf was used for the hardness measurements. The machined samples contained the recast layer on mild steel, with an average thickness of 40 μm . The hardness of the matrix is 184-220 HV. In addition, the hardness of the recast layer machined with graphite electrode was higher than that of the recast layer machined with copper electrode. The microhardness of the recast layer with

graphite electrode reached 420 HV, which is a little higher than that of machined with copper electrode (320HV). This is attributed to the higher carbon content on the cast layer. The dendritic which has a needle structure can be seen in Fig. 2(b). In this case, carbon is transferred from the graphite electrode and the white layer freeze to martensitic structure [14].

The relationship between the surface roughness of EDMed surface treated by graphite and copper electrode are presented in Fig 5. The surface roughness that produced with graphite electrode was higher than that of copper electrode. This phenomenon may explain that graphite powder from graphite electrode make pores to the layer and make rougher than that EDMed with copper.

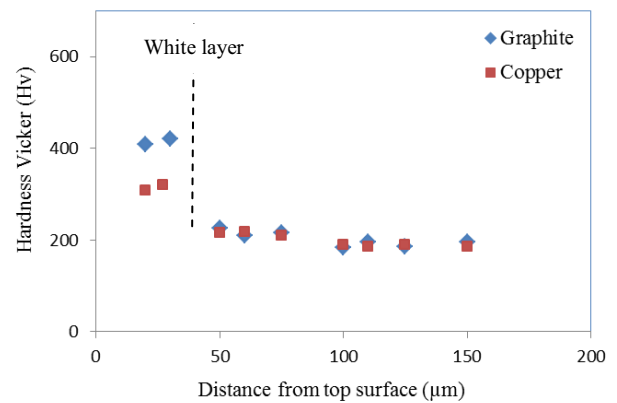


Figure 4. Microhardness distribution of the cross section of layers treated by EDM.

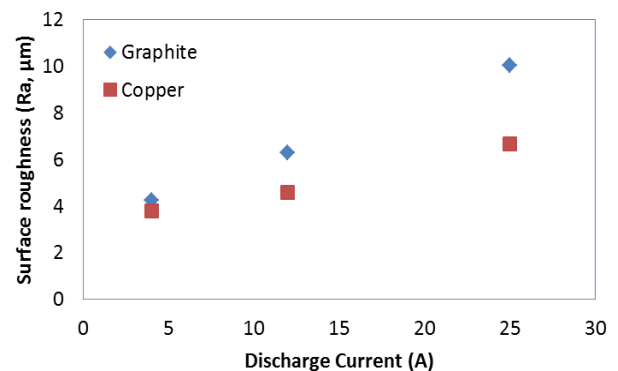


Figure 5. Surface roughness of gray iron and mild steel surfaces treated by EDM in different media.

4 Conclusion

1. There is no crack on white layer when EDM with graphite electrode.
2. Carbon from electrode material regenerate to the white layer.
3. Carbon can be found on EDMed surface with graphite electrode. However, it is not enough to generate to Fe_3C .
4. Graphite electrode make more surface roughness than that made by copper electrode.

Acknowledgements

The authors acknowledge the support from the Thammasat University research's fund, the Commission on Higher Education of Thailand (the National Research University Project).

References

1. Y. Zhang, Y. Liu, Y. Shen, R. Ji, Z. Li, C. Zheng, J. Mater. Process. Technol., **214**, 5, 1052–1061 (2014)
2. M. Barash, M. G. Sri-Ram, Proceedings of Third International Machine Tool Design and Research Conference, 85–91, Birmingham (1962)
3. J. C. Rebelo, A. M. Diaz, D. Kremer, J. L. Lebrun, J. Mater. Process. Technol., **84**, 1–3, 90–99 (1998)
4. B. Ekmekci, Metall. Mater. Trans. B, Process., Sci. **40**, 70–81 (2009)
5. J. P. Kruth, L. Stevens, L. Froyen, B. Lauwers, K. U. Leuven, Ann. CIRP, **44**, 169–172 (1995)
6. F. L. Amorim, W. L. Weingaertner, J. Braz., Soc. Mech. Sci. & Eng., **29**, 4 (2007)
7. H. T. Lee, T. Y. Tai, J. Mater. Process. Technol., **142**, 3, 676–683(2003)
8. S. L. Chen, B. H. Yan, F. Y. Huang, J. Mater. Process. Technol., **87**, 107–111 (1999)
9. G. Cusanelli, A. Hessler-Wyser, F. Bobard, R. Demellayer, R. Perez, R. Flükiger, J. Mater. Process. Technol., **149**, 289–295 (2004)
10. F. J. O'Brien, D. Taylor, T. C. Lee, J. Biomech., **36**, 973–980 (2003)
11. F. Ghanem, C. Braham, H. Sidhom, J. Mater. Process. Technol., **142**, 163–173 (2003).
12. J. P. Kruth, J. V. Humbeeck, L. Stevens, Proceedings of the ISEM XI, 849–862 (1995)
13. E. D. Cabanillas, J. Desimoni, G. Punte, R. C. Mercader, Mater. Sci. Eng. A, 276, 133–140 (2000)
14. M. Barash, Metals Eng., **5**, 48–51 (1965)